IN-47-CR
5420
P 10

Project NAG-1-1062: Final Technical Report

Analysis of Energy Balance Models Using the ERBE Data Set

Dr. Charles E. Graves and Dr. Gerald R. North

Climate System Research Program
Department of Meteorology
Texas A&M University
College Station, Texas 77843

3 April, 1991

(NASA-CR-188002) ANALYSIS OF ENERGY BALANCE MODELS USING THE ERBE DATA SET Final Report (Texas A&M Univ.) 10 p CSCL 04B

N91-20596

Unclas
G3/47 0005420

1 Introduction

The research associated with the project **"Analysis of Energy Balance Models Using the ERBE Data Set"** is essentially completed. The majority of the ongoing work is the preparation of two manuscripts for publication. When the manuscripts are completed they will be forwarded. The basic contents of the manuscripts are discussed below. The research has lead to confirmation of previous work as well as a more quantitative understanding of the role of clouds in energy balance models.

This report is divided into four sections. The first is a review of Energy Balance Models (EBMs). The second discusses results from the Outgoing Longwave Radiation (OLR) parameterization. The third section examines the albedo parameterizations, while the last section examines the consequences of these new parameterizations.

2 Review

Since the introduction of Energy Balance Models (EBMs) by Budkyo (1968, 1969) and Sellers (1969) they have become a useful tool for analyzing climate and climate change. The EBM is a phenomenology model describing the local energy balance as a sum of terms, each dealing with a separate flux:

(energy storage rate) + (divergence of horizontal heat flux)
+ (energy radiated away) = (solar energy absorbed)

The EBMs are viewed as an ensemble average of the seasonal cycle similar to ensemble averages in statistical mechanics. The steady state solution represents the average of many independent earths, each one started from a different set of initial conditions. The steady state solution is thus an "average weather pattern" or an estimate of the climatic state.

The EBM version relevant to this project which includes seasonal forcing and two dimensional geography is governed by the equation:

$$C\frac{\partial T}{\partial t} - \nabla \cdot (D\nabla T) + A + BT = QaS.$$

Where T is the surface temperature and

$C\,\partial T/\partial t$ is the local energy change, C being the effective heat capacity

$\nabla \cdot (D\nabla T)$ is the horizontal divergence of heat flux, using a diffusion approximation

$A + BT$ is the representation of outgoing radiation

QaS is the insolation $\times$ co-albedo; the amount of energy absorbed by the system.

The effective heat capacity, C, represents the local effective heat capacity of the earth-atmosphere system. It has separate values over land and ocean, being about 60 times larger over the oceans indicative of the larger heat storage in the mixed layer of the oceans. The diffusion coefficient has a latitudinal dependence decreasing in value away from the equator, indicating less efficient energy transport away from the equator. The values for A, B, as well as the latitudinal shape and magnitude of the co-albedo, a, are derived from satellite data (Short et al., 1984). The normalized solar insolation, S is determined by celestial mechanics; to a good approximation this can be written as a truncated Fourier series in time and a truncated Legrendre polynomial in latitude (North and Coakley, 1979). Typical numerical values and spatial dependence of all these coefficients is discussed further by North et al (1983).

The EBM can be made nonlinear by allowing the co-albedo to change with surface temperature. In particular, the albedo changes if the temperature falls below zero, representing the change in albedo due to snow. This snowline feedback leads to a very interesting an aspect of EBMs which is currently being investigated (Mengel et al 1988; Lin and North 1989).

Considering that the key elements of the earth's climate fluxes have been represented almost schematically, EBMs have been notably successful at reproducing the past and present climate of earth. Several studies have demonstrated the ability of EBMs to reproduce the current annual cycle (e.g., North et al 1983). However, the EBM produces a smoother structure in the phase of the annual cycle than observed. The EBM phase is mainly determined by the type of surface; oceans have 90 day phase lag while the land has about a 30 day phase lag (i.e. the phase is mainly determined by the value of C).

3 Outgoing Longwave Radiation Results

The OLR parameterization coefficients A and B were estimated from three different data sets of monthly mean OLR data along with an updated version of the monthly mean surface temperature data used by Jones et al. (1984). (The temperature data were kindly provided by NCAR). One of the OLR data sets is from 10 years of wide field of view radiometers aboard

Nimbus 6 and 7 which were obtained from Bess and Smith (1987a, 1987b). The other two data sets are nine months of ERBE average sky and ERBE clear sky measurements and were obtained from NESDIS.

With regard to climate sensitivity, B is the parameter of interest since it governs the rate at which anomalies are radiatively damped (radiative damping time is C/B and C is fixed by geography). Also the sensivity to static changes in other external variables such as the solar constant is proportional to $1/B$. Thus, this report will concentrate on the estimates of B obtained from the data by linear regression.

Both the 10 year and ERBE average sky data sets produced nearly the same estimates of B. The estimates of B from the 10 year data set are presented in Fig. 1a. In the middle and high latitudes B has nearly a constant value of 2.0 W m^{-2} C^{-1}. In contrast, B has considerably more variability in the tropics. This variability simply reflects the strong local cloud–OLR relationship that is commonly exploited throughout much of the tropics. In these regions a warmer surface temperature is more closely related to increased cloudiness, hence a decrease in OLR rather than the increase observed in the higher latitudes.

However, when examining the estimates of B derived from the clear sky OLR values (shown in Fig. 1b) the results are quite different. The highly variable nature of B is no longer observed in the tropics. The observed variability is more akin to that found in the average sky case throughout the middle and high latitudes. Moreover, the value of the clear sky B is generally larger (closer to 2.2 W m^{-2} C^{-1}) agrees better with radiative transfer calculations (Cess, 1974).

Typically, EBMs employ a constant value of B, and as shown in Fig. 1, there is scatter in the value of B even in the middle and high latitudes. The scatter for the 10 year and clear sky OLR data are presented in 2-D histograms in Fig 2a and 2b respectively. (These histograms contain area weighting to refect the larger surface areas in the lower latitudes.) The scatter of B in Fig 2a hints at a quadratic nature to the relationship between surface temperature and OLR which is not found in the clear sky case (Fig. 2b). However, the quadratic coefficient obtained from a least square estimate was quite small, about 0.01 W m^{-2} C^{-2} which is not significant. Finally, the mean value for B estimated from the 10 year OLR data is 1.90 W m^{-2} C^{-1}, which is very close to the 1.93 W m^{-2} C^{-1} found from 1 year of data by Short et al (1984)

Additional temporal information was examined with the 10 year OLR data set. From cross spectral analysis, the relationship between the surface temperature and OLR is strongest at the annual cycle and only meager at other frequencies. Furthermore, the annual cycle accounted for a large fraction (nearly 90%) of the entire variance for both the OLR and

temperature. The strong relationship between OLR and temperature at the annual cycle versus the weak relationship at the other frequencies is reminiscent of the forced and free oscillations discussed by Lorenz (1979).

4 Albedo Results

The analysis of the albedo was more involved and its details will be presented elsewhere. The albedo estimates (or co-albedo as used in EBMs) were obtained from the same 9 months of ERBE OLR data. The EBM model for co-albedo is:

$$c \cdot (a_0 + a_1 \cdot P_1(\text{latitude}))$$

Which represents a truncated Legrendre polynomial expansion of the total co-albedo. (P_1 is the Legrendre polynomial of order 1). The multiplicative constant, c represents the change in co-albedo due to snow. Previous studies contained fixed coefficients and c arbitrarily changed from a value of 1 to 0.5 to mimic the reduced energy absorption in the presence of snow. (In an EBM, snow is present on the surface if the temperature drops below some threshold like 0 C.)

In the current study, similar values for the coefficients a_0 and a_1 were obtained however they also contain a small time dependence indicative of the change in solar geometry. However, the transition from snow to no snow is smeared out due to clouds and can be difficult to determine. The present best estimate is that C change from 1 to 0.4, a slightly larger transition that previously used. In the clear sky analysis, the coefficients a_0 and a_1 increase slightly causing greater solar absorption and the transition from no snow to snow was much more dramatic. The transition was from 1 to 0.25 (rather than a change from 1 to 0.4). An example showing the difference between the average and clear sky albedos is in zonal averaged albedos shown Fig. 3. The transition region becomes smeared due to the zonal average, however a indication of the dramatic change in the no snow – snow transition from average to clear skies can be observed.

5 Conclusions

The final OLR and albedo parameters obtained in this study which are suitable for EBMs arre generaly consistent with previous values. However we have obtained additional justification

for the size of the transition coefficient c, which denotes the change in albedo from no snow to snow.

In comparing the average sky results with the clear sky results we have found that clouds increase the variability of the OLR temperature relationship. This additional "scatter" is removed in the ensemble averaged framework of the EBM. Furthermore this amount of scatter can be utilized as noise in the noise forced EBM. The characterization of this "noise" is an interesting and possibly fruitful study. Furthermore the effect of clouds acts to decrease the value of B by about 0.4 W m^{-2} C^{-1}, hence reducing the amount of energy emitted to space (the OLR warming effect of clouds). In contrast, the albedo increases by 10% or more, and results in less energy being absorbed (the albedo cooling effect of clouds). There is significant cancelation between these two effects. While the ERBE team has found the net effect of clouds is a 17 W m^{-2} cooling (Ramanathan et al., 1989), it will be interesting to determine the net effect from the EBM. (These results are just being processed and will be included in the forthcoming manuscript.)

References

- Bess T. D. and G. L. Smith, 1987a: *Atlas of the wide-field-of-view outgoing long-wave radiation form Nimbus 6 earth radiation budget data set - July 1975 to June 1978*, NASA RP-1185.
- Bess T. D. and G. L. Smith, 1987b: *Atlas of the wide-field-of-view outgoing long-wave radiation form Nimbus 7 earth radiation budget data set - November 1978 to October 1985*, NASA RP-1186.
- Budydko, M. I., 1968: On the origins of glacial epochs, *Meteorol. Gidrol*, **2**, 3-8.
- Budydko, M. I., 1969: The effect of solar radiation variations on the climate of the earth, *Tellus*, **21**, 611-619.
- Cess R. D., 1974: Radiative transfer due to atmospheric water vapor: Global considerations of the earth's energy balance, *J. Quant. Spectrosc Radiat. Transfer*, **14**, 861-871.
- Jones P. D., T. M. Wigley, and P. M. Kelly, 1982: Variations in surface air temperatures: Part I: Northern Hemisphere, 1881-1980. *Mon. Wea. Rev.*, **110**, 59-70.
- Lin, R-Q and G. R. North, 1989: A study of abrupt climate change in a simple nonlinear climate model. Submitted to *J. Atmos. Sci.*

- Mengel, J. G., D. A. Short, and G. R. North, 1988: Seasonal snowline instability in an energy balance model, *Climate Dyn.*, **2**, 127-131.
- North, G. R., 1975: Analytical solution to a simple climate model with diffusive heat transport, *J. Atmos. Sci.*, **32**, 1301-1307.
- North, G. R., 1975: Theory of energy balance models, *J. Atmos. Sci.*, **32**, 2033-2043.
- North, G. R., 1984: The small ice cap instability in diffusive energy balance models, *J. Atmos. Sci.*, **41**, 3390-3395.
- North, G. R., 1988: Lessons from energy balance models, *Physically-based Modelling and Simulation of Climate and Climate Change - Part II*, Ed. M. E. Schlesinger, 627-651.
- North, G. R. and J. A. Coakley, 1979: Differences between seasonal and mean annual energy balance model calculations of climate and climate sensitivity, *J. Atmos. Sci.*, **36**, 1189-1204.
- North, G. R., R. F. Cahalan and J. A. Coakley Jr., 1981: Energy balance models, *Rev. Geophys. Space Phys.*, **19**, 91-121.
- Ramanathan, V., B. R. Barkstrom, and E. F. Harrison, 1989: Climate and the earth's radiation budget, *Physics Today*, May, 22-32.
- Sellers, W. D., 1969: A climate model based on the energy balance of the earth-atmosphere system, *J. Appl. Meteor.*, **8**, 392-400.
- Sellers, W. D., 1970: The effect of changes in the earth's obliquity on the distribution of mean annual sea-level temperatures. *J. Appl. Meterol.*, **9**, 960-961.
- Sellers, W. D., 1973: A new global climate model, *J. Appl. Meterol.*, **12**, 241-254.
- Sellers, W. D., 1976 A two-dimensional global climate model, *Mon. Wea. Rev.*, **104**, 233-248.
- Short D. D., G. R. North, T. D. Bess, and G. L. Smith 1984: Infrared parameterization and simple climate models, *J. Clim. Appl. Meteor.*, **23**, 1222-1233.

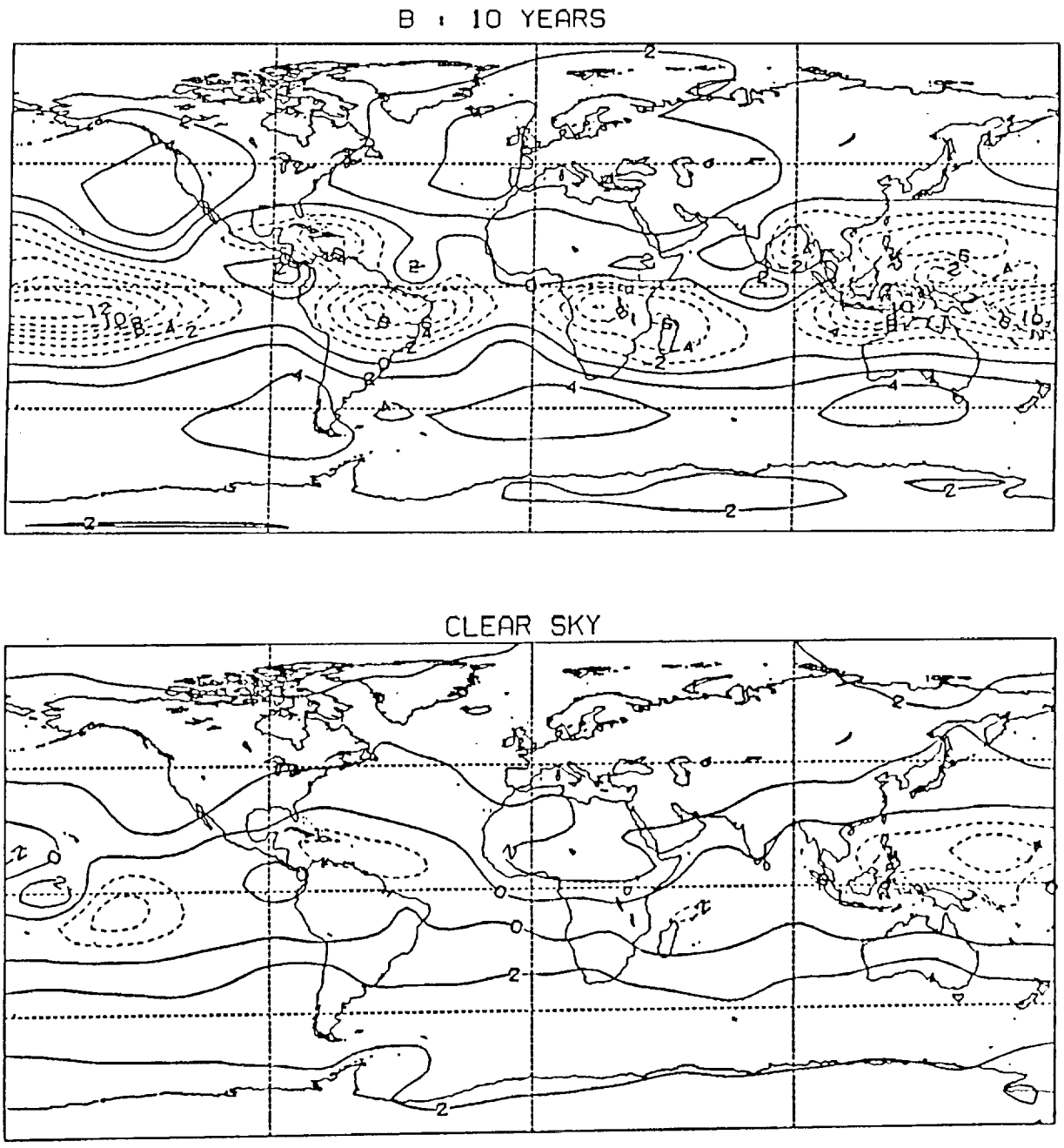

Figure 1: The estimate of B from a)the 10 year OLR data set and b)the ERBE clear sky data set. The contour levels are in increments of 2 W m^{-2} C^{-1}. The effective resolution of the plot is about 15° × 15°.

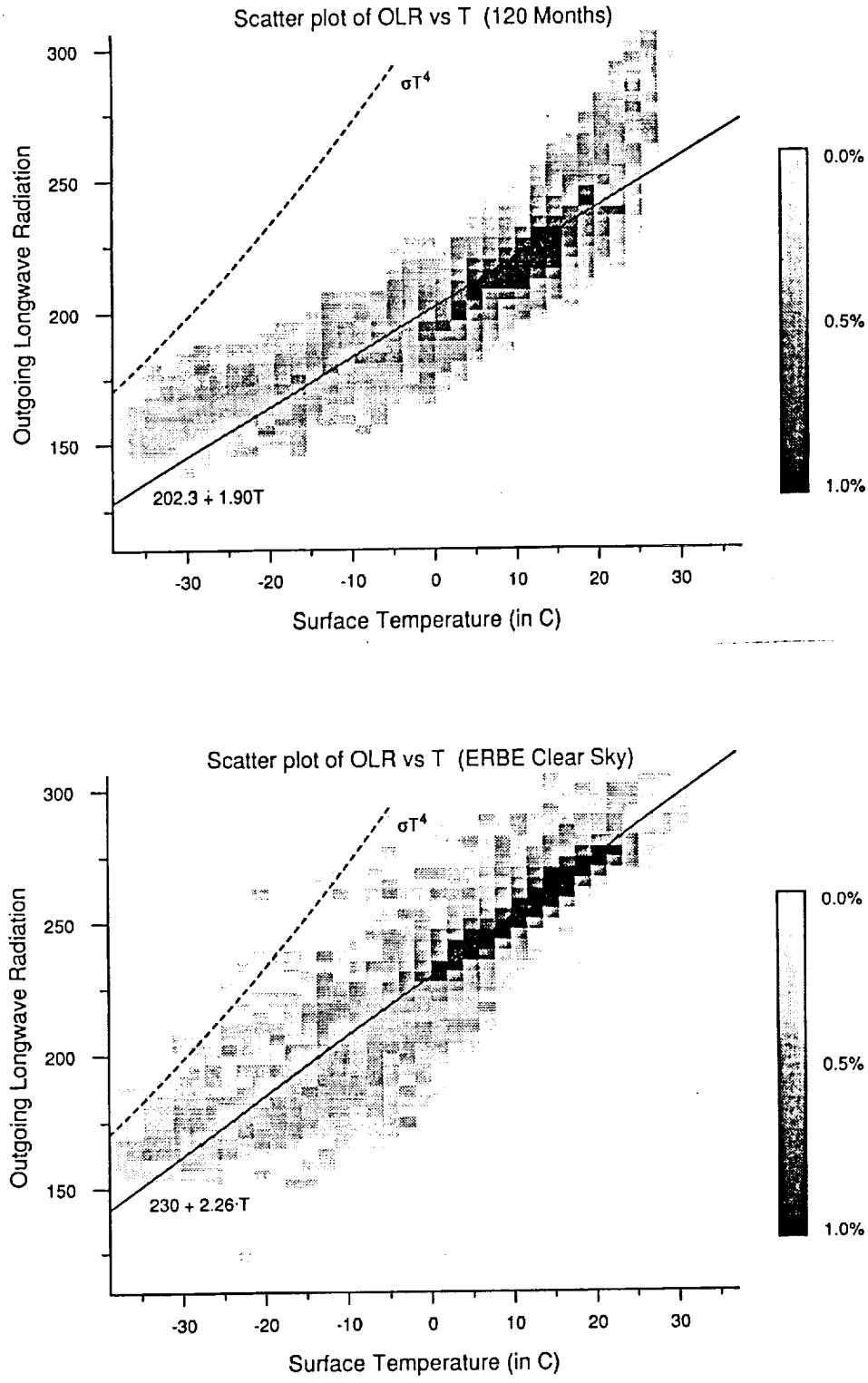

Figure 2: 2-D histograms for a)the 10 year OLR data set and b)the ERBE clear sky data set, which represent scatter diagrams. Each bin represents the fraction of total area found with in that particular OLR and temperture bin. The scale on the right indicates the percent of total area. The solid line represents the linear fit to this scatter and the dashed line represents the Stefan-Boltzman law (σT^4)

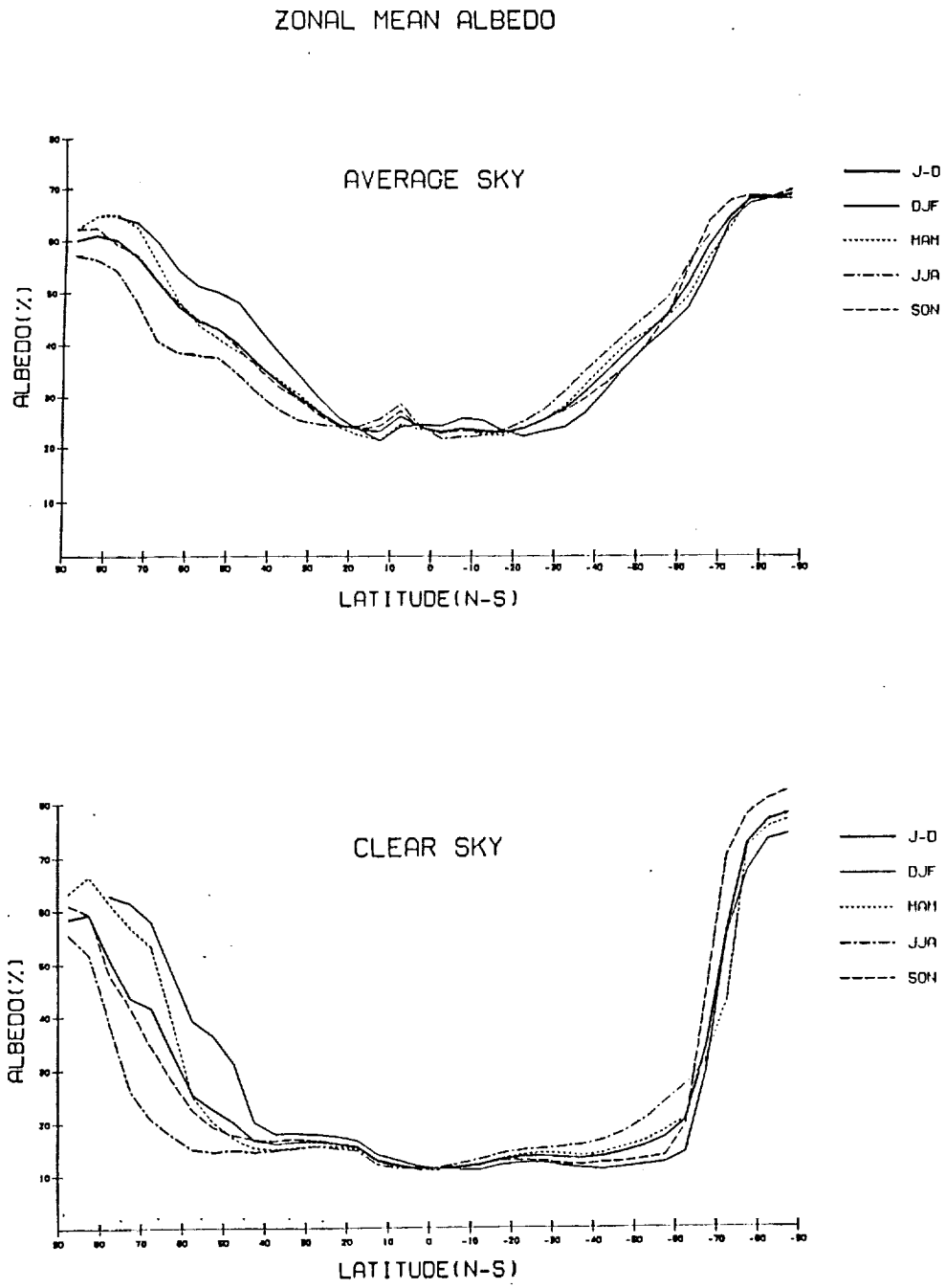

Figure 3: Zonally average albedo from a)the ERBE average sky data set and b)the ERBE clear sky data set. The albedo is in percent and the different line types represent the different seasonal averages (i.e. DJF - average over December, January, Feburary, etc.)